AD NUMBER

AD909437

LIMITATION CHANGES

TO:

Approved for public release; distribution is unlimited.

FROM:

Distribution authorized to U.S. Gov't. agencies only; Test and Evaluation; 13 APR 1973. Other requests shall be referred to Department of the Army Attn: DARD-ZCA, Washington, DC 20310.

AUTHORITY

DA ltr 10 Aug 1973

TO ASAP

AD-909437-L

EMPLOYMENT OF A SPIN STABILIZED ARTILLERY SHELL TO OBTAIN RECONNAISSANCE IMAGERY

Paul W. Kruse
Army Scientific Advisory Panel
June, 1971

per Cl. Barbules 69-57487

Distribution limited to U.S. Gov't. agencies only; Test and Evaluation; 4-13-73 . Other requests for this document must be referred to

HQDA (DARD-ZCA)
WASH., D.C. 20310

RN
4-13-73

EMPLOYMENT OF A SPIN STABILIZED ARTILLERY SHELL TO OBTAIN RECONNAISSANCE IMAGERY

Paul W. Kruse
Army Scientific Advisory Panel

June, 1971

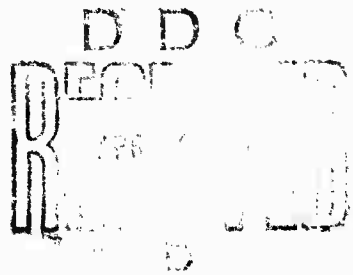

ABSTRACT

The concept of employing an expendable spin stabilized artillery shell containing a simple optical system to obtain reconnaissance imagery has been suggested by Dr. Marvin Lasser. This paper provides an initial examination of the technical feasibility of the concept. Three geometrical scanning configurations are considered; a side-looking one is analyzed in detail. The requirement for time independent contiguous mapping, in which each scanning line must touch its neighbors, is analyzed. Data on the ballistics of a 203mm round fired at a 45° angle to a range of 16,700 meters are introduced into the equations. It is found that for this particular trajectory the time independent contiguous mapping requirement can be met over a 1 kilometer horizontal distance near apogee. The ground resolution for this trajectory is found to be sufficiently good for use against targets such as vehicles, buildings, roads, and groups of individuals which lie beneath the round at apogee. Analysis of photometric considerations reveals adequate signal-to-noise ratio for use beneath a cloud cover during daylight. Because the initial examination reveals the concept to be feasible, additional studies are recommended.

TABLE OF CONTENTS

		Page
1.0	INTRODUCTION	1
	1.1 Statement of the Problem	1
	1.2 Ballistic Data	2
2.0	OPTICAL CONFIGURATIONS	6
	2.1 Description	6
	2.2 Discussion	9
3.0	PERFORMANCE CALCULATIONS	12
	3.1 Geometrical Considerations	16
	3.1.1 Time Independent Contiguous Mapping	16
	3.1.2 Dwell Time	23
	3.1.3 Ground Resolution	24
	3.2 Photometric Considerations	27
	3.2.1 Properties of Silicon Photocells	28
	3.2.2 Signal-to-Noise Ratio and Minimum Detectable Contrast	30
4.0	DISCUSSION AND SUMMARY	35
5.0	RECOMMENDATIONS	37
	REFERENCES	39

LIST OF FIGURES

FIGURE		PAGE
1.	TRAJECTORY OF 203MM ROUND	4
2.	DEPENDENCE OF ASPECT ANGLE UPON RANGE	5
3.	DEPENDENCES OF SPIN RATE AND HORIZONTAL COMPONENT OF VELOCITY UPON RANGE	7
4.	SIDE LOOKING CONFIGURATION	8
5.	FORWARD LOOKING CONFIGURATION	10
6.	AXIAL CONFIGURATION	11
7.	INTERSECTION OF FIELD OF VIEW OF SIDE LOOKING CONFIGURATION WITH EARTH PLANE	13
8.	INTERSECTION OF FIELD OF VIEW OF FORWARD LOOKING CONFIGURATION WITH EARTH PLANE-PARABOLIC CASE	14
9.	INTERSECTION OF FIELD OF VIEW OF FORWARD LOOKING CONFIGURATION WITH EARTH PLANE-ELLIPTICAL CASE	15
10.	INTERSECTION OF FIELD OF VIEW WITH EARTH PLANE (TRACK) AS A FUNCTION OF HORIZONTAL DISTANCE OF SHELL FROM LAUNCH POINT (RANGE)	19
11.	DEPENDENCE OF $V_T \cos^2\theta_D/hr$ UPON RANGE	21
12.	SCANNING GEOMETRY PERPENDICULAR TO FLIGHT PATH	25
13.	GROUND RESOLUTION AS A FUNCTION OF RANGE	26
14.	SPECTRAL RESPONSE OF SILICON PHOTODIODE; SOLAR SPECTRUM AT SURFACE OF THE EARTH	29
15.	GEOMETRY FOR PHOTOMETRIC ANALYSIS	31

LIST OF TABLES

TABLE		PAGE
1.	BALLISTIC DATA: STANDARD 203MM M106 ROUND, ZONE 7, MUZZLE VELOCITY 1950 FT/SEC, WEIGHT 200 LBS., ZERO WIND, 45° ELEVATION, FIRED NORTH FROM EQUATOR AT SEA LEVEL, IMPACT AT SEA LEVEL	3
2.	VALUES OF PERTINENT PARAMETERS CALCULATED FROM DATA IN TABLE 1	18

EMPLOYMENT OF A SPIN STABILIZED ARTILLERY SHELL TO OBTAIN RECONNAISSANCE IMAGERY

Paul W. Kruse
Army Scientific Advisory Panel

1.0 INTRODUCTION

1.1 Statement of the Problem

Dr. Marvin Lasser, Chief Scientist, U. S. Army, has suggested employing a spin stabilized artillery shell containing an optical system to obtain reconnaissance imagery of terrain. The concept involves use of the spin to provide a scanning action similar to that of an aircraft-mounted mechanically scanned strip mapper. That is to say, as the round spins in flight, the field of view of the optical system looking outward describes a spiral in space which intercepts the earth plane. Point-to-point variations in the solar radiation reflected from the earth (or thermal radiation emitted by the earth) which are intercepted by the scanning system and focused on a photocell cause a time dependent photo-signal. This signal is telemetered back to a station near the firing site, where the imagery is reconstructed to provide a photo of the terrain overflown.

Because each round fired would be destroyed, a key requirement is low unit cost. If cost were no consideration, a fin stabilized projectile mounting a TV camera could be employed. The spinning round concept must result in a much less expensive approach. Ideally, a round having the same ballistic properties as a conventional H. E. round would employ inexpensive optics, solid state photosensors, and integrated circuits in place of the safing, arming, fuzing, and explosive sections. Relatively expensive components such as gyros and gimbals would not be used. Complexity, if required, would be in the ground based telemetry receiver, imagery decoder, and display, rather than in the round itself.

This paper constitutes a first look at the problem. It presents a simplified analysis which identifies those areas requiring more detailed studies. Both the geometric and the photometric aspects of the problem

are considered, i.e., the manner by which the spinning optics scan a resolution element over the terrain, and the resulting signal-to-noise ratio of the photocell output. The telemetry aspect is ignored; the analysis assumes that the data provided in the output from the photocell can be telemetered without degradation to a receiving station located near the artillery piece which fired the round. Other questions such as the effect of the firing shock upon the optical and electronic equipment are also ignored. It is assumed that the round would be used only in the daytime, so that the photosignal arises from reflected solar radiation rather than emitted thermal radiation. Obviously an analysis in much greater depth is required before the true feasibility of the concept can be determined.

1.2 Ballistic Data

To serve as a model to determine feasibility, ballistic data have been obtained[1] on the standard 203mm M106 round fired due north from the equator in the absence of wind with a zone 7 charge at 45° elevation, see Table 1. No significance should be attached to the choice of caliber or firing conditions. It seems likely that a large round, 155mm, 175mm, or 203mm, would be required to contain the optical system. The firing conditions were selected as being a reasonable choice for use in the calculations. It is obvious that a large number of other reasonable choices could have been made.

Among other interesting observations, the data show that the yaw, i.e., the deviation of the spin vector from the velocity vector, has a maximum value of only 1.29°. Thus it will be assumed that yaw can be neglected, so that the spin vector is always aligned with the velocity vector, both being tangent to the trajectory at each instant.

Figure 1 illustrates the trajectory. Fired at 45° elevation, the round reaches an apogee of about 5202 meters at a range of about 9100 meters about 30 seconds after firing. Impact occurs 64.3 seconds after firing at a range of about 16,700 meters.

Figure 2 illustrates the range dependence of the aspect angle θ_D which the

TABLE 1

BALLISTIC DATA: STANDARD 203MM M106 ROUND, ZONE 7, MUZZLE VELOCITY 1950 FT/SEC, WEIGHT 200 LBS., ZERO WIND, 45° ELEVATION, FIRED NORTH FROM EQUATOR AT SEA LEVEL, IMPACT AT SEA LEVEL

Time (Seconds)	Horizontal Range (Meters)	Altitude (Meters)	Crosstrack (Meters)	Horizontal Velocity (Meters/Sec)	Vertical Velocity (Meters/Sec)	Velocity (Meters/Sec)	Θ_D (Degrees)	Yaw (Degrees)	Spin (Radians/Sec)
0.0	0.0	0.0	0.0	420.3	420.3	594.4	45.0	0.0	735.00
2.2	885.8	862.8	0.3	386.3	365.6	531.8	43.4	0.08	720.39
4.4	1704.4	1614.7	1.2	358.9	319.0	480.2	41.6	0.12	708.05
6.6	2468.7	2271.0	2.9	336.6	278.2	436.7	39.6	0.16	697.52
8.8	3188.1	2842.8	5.5	317.9	241.9	399.5	37.3	0.22	688.35
11.0	3869.7	3338.6	9.0	302.2	209.0	367.4	34.7	0.30	680.22
13.2	4519.3	3765.1	13.5	288.8	178.8	339.7	31.8	0.39	672.88
15.4	5142.8	4128.1	18.9	278.5	151.3	316.9	28.5	0.51	666.15
17.6	5746.8	4433.3	25.3	271.1	126.1	299.0	24.9	0.64	659.89
19.8	6337.4	4684.9	32.6	266.0	102.4	285.1	21.1	0.80	653.99
22.0	6918.3	4885.8	40.9	262.3	79.7	274.1	16.9	0.94	648.36
24.2	7491.8	5037.1	50.3	259.2	57.4	265.5	12.5	1.06	642.96
26.4	8058.8	5140.0	60.8	256.4	35.5	258.9	7.9	1.17	637.71
28.6	8620.0	5194.9	72.5	253.8	13.8	254.2	3.1	1.25	632.59
30.8	9175.4	5202.3	85.4	251.2	-7.7	251.4	-1.7	1.29	627.59
33.0	9725.2	5162.9	99.6	248.7	-28.9	250.4	-6.6	1.28	622.66
35.2	10269.5	5076.9	115.0	246.2	-50.0	251.3	-11.5	1.23	617.73
37.4	10808.3	4944.8	131.7	243.6	-70.8	253.8	-16.2	1.14	612.75
39.6	11341.5	4767.3	149.6	241.1	-91.4	258.0	-20.8	1.03	607.67
41.8	11868.9	4544.7	168.7	238.4	-111.8	263.5	-25.1	0.90	602.46
44.0	12390.5	4277.6	188.8	235.7	-131.8	270.2	-29.2	0.77	597.12
46.2	12905.6	3966.9	210.1	232.6	-151.5	277.7	-33.1	0.65	591.61
48.4	13413.4	3613.7	232.3	229.0	-170.5	285.7	-36.6	0.55	585.89
50.6	13912.8	3219.5	255.4	224.8	-188.7	293.7	-40.0	0.46	579.94
52.8	14401.9	2786.6	279.5	219.7	-205.7	301.2	-43.1	0.38	573.72
55.0	14879.0	2317.5	304.3	213.9	-221.5	308.1	-46.0	0.31	567.20
57.2	15342.4	1815.2	330.0	207.3	-235.9	314.2	-48.6	0.26	560.36
59.4	15790.5	1282.9	356.5	200.0	-248.8	319.4	-51.2	0.22	553.18
61.6	16222.0	723.9	383.7	192.2	-260.2	323.7	-53.5	0.19	545.62
63.8	16635.8	141.2	411.7	184.0	-270.2	327.2	-55.7	0.16	537.68
64.3	16729.6	0.0	418.4	182.0	-272.4	327.9	-56.2	0.15	535.77

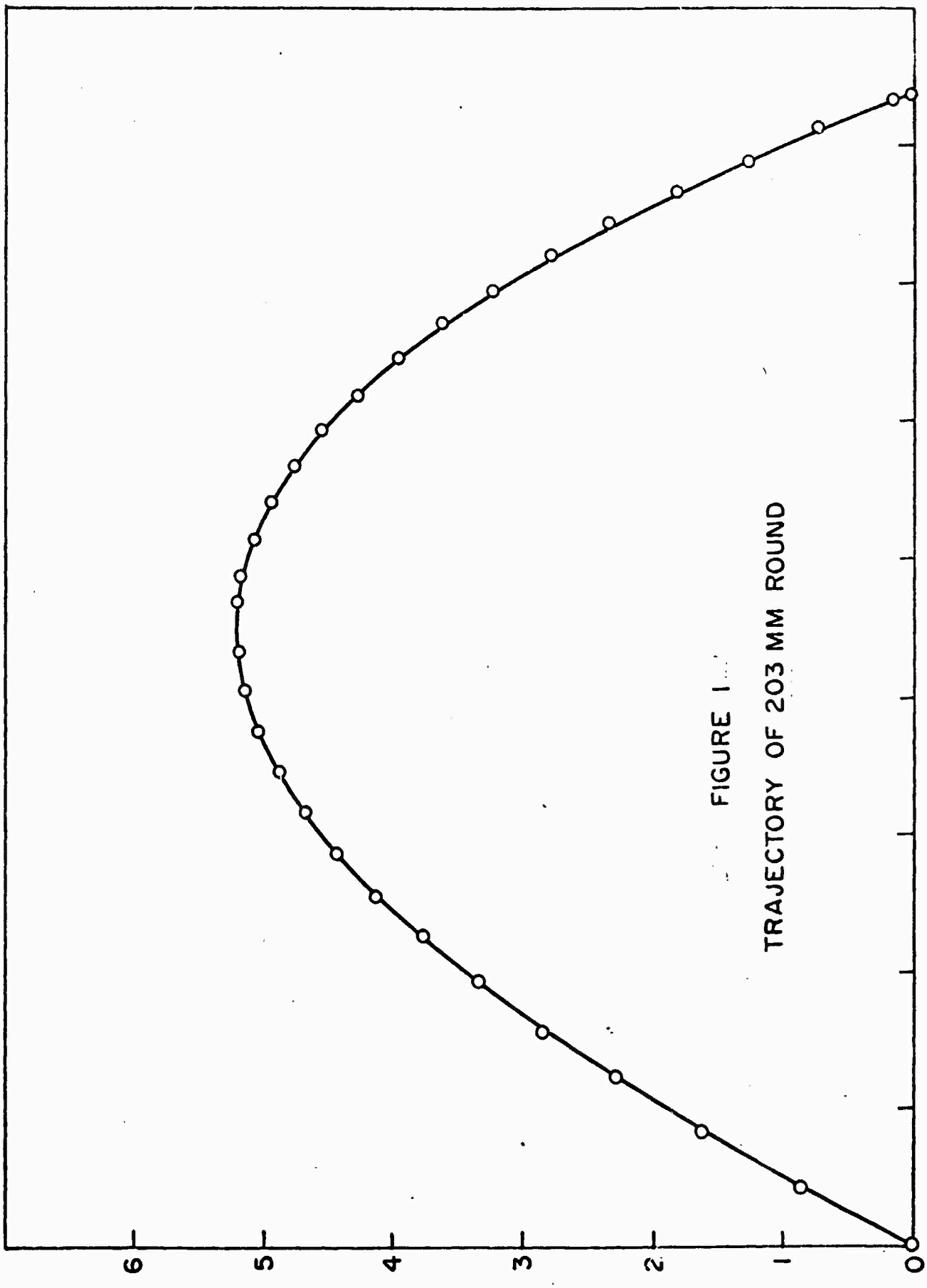

FIGURE 1

TRAJECTORY OF 203 MM ROUND

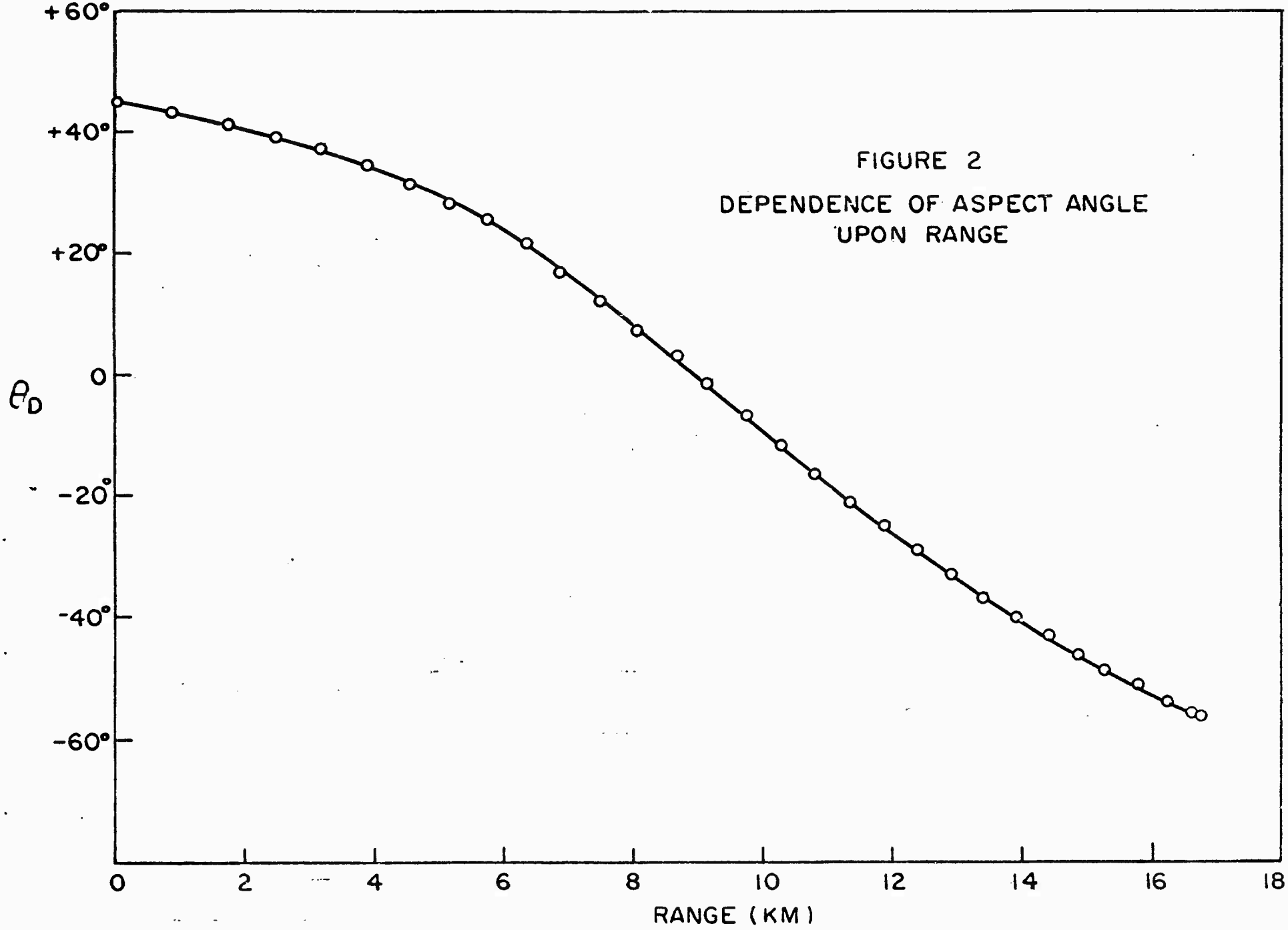

FIGURE 2

DEPENDENCE OF ASPECT ANGLE UPON RANGE

shell axis makes with respect to the horizontal. The angle, tangent to the trajectory, changes continuously with respect to range. Thus the angle which the field of view makes with the ground plane also changes continuously with time.

Figure 3 illustrates the dependence of the horizontal velocity component and the spin rate upon range. Both velocity and spin decrease monotonically with range, and therefore, with time.

It is clear, therefore, that all the important parameters change continuously with time. From this it is concluded that two types of operation are possible.

A. Operate only during any portion of the trajectory in which these time dependences tend to compensate for each other.

B. Measure independently these time dependent parameters and telemeter the values to the receiving station. Employ a computer to reconstruct the imagery from knowledge of the parameter values and time dependent photosignal.

Obviously it is much more simple to operate in mode A than mode B. Accordingly, the thrust of this analysis will be to examine the ballistic data in light of the scanning model to be developed, then ascertain which, if any, portions of the trajectory allow for mode A operation. If any portion does, then operation of the scanner during that portion will be considered in detail.

2.0 OPTICAL CONFIGURATIONS

2.1 Description

There are three optical configurations which are envisioned:

A. A "side looking" one in which the field of view is normal to the axis of the shell, see Fig. 4. In this configuration the optical system would be mounted, say, halfway back from the nose. The round might be contained within a sabot discarded after

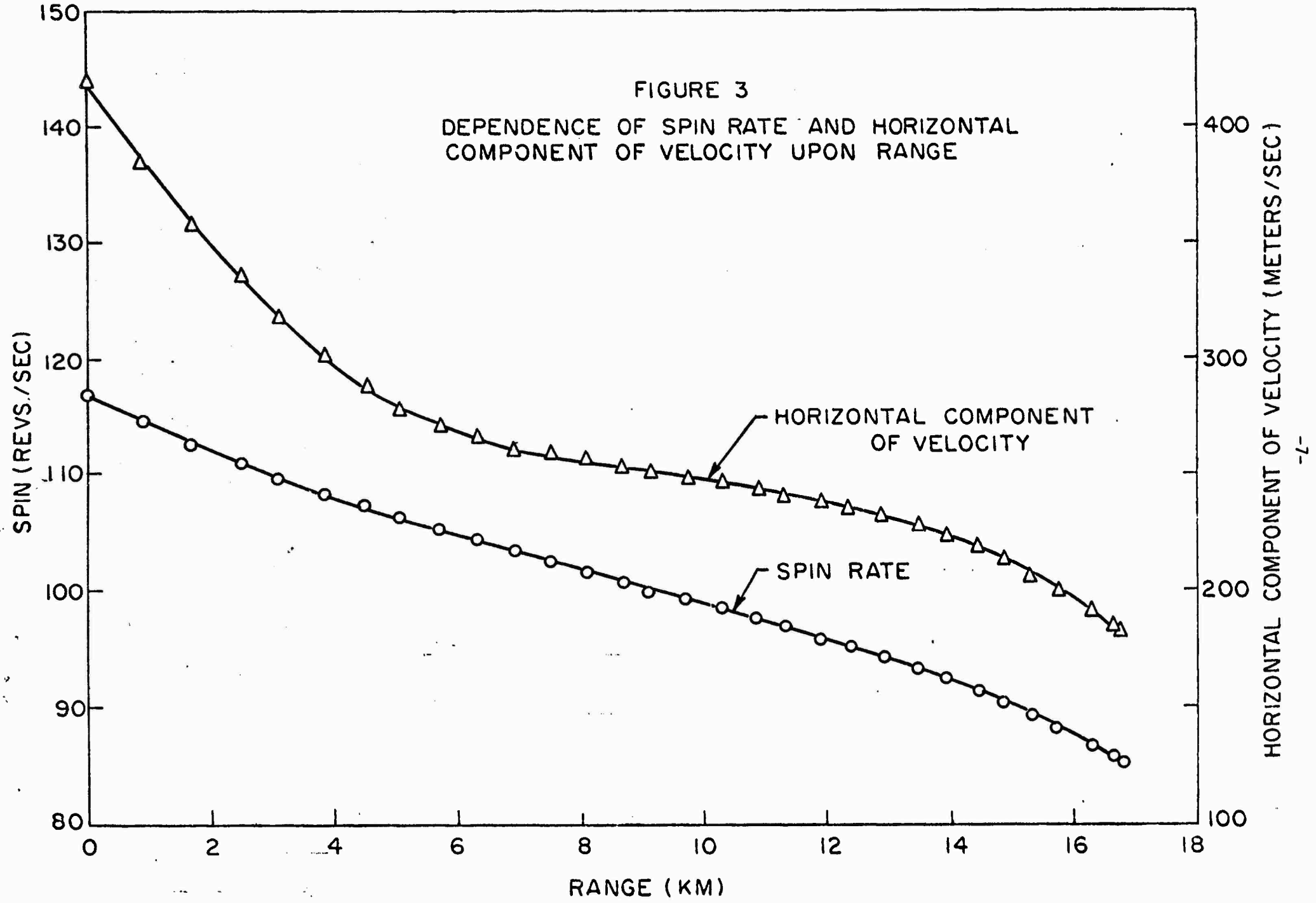
FIGURE 3
DEPENDENCE OF SPIN RATE AND HORIZONTAL COMPONENT OF VELOCITY UPON RANGE
SPIN (REVS./SEC)
HORIZONTAL COMPONENT OF VELOCITY (METERS/SEC)
RANGE (KM)
HORIZONTAL COMPONENT OF VELOCITY
SPIN RATE
150
140
130
120
110
100
90
80
400
300
200
100
0
2
4
6
8
10
12
14
16
18

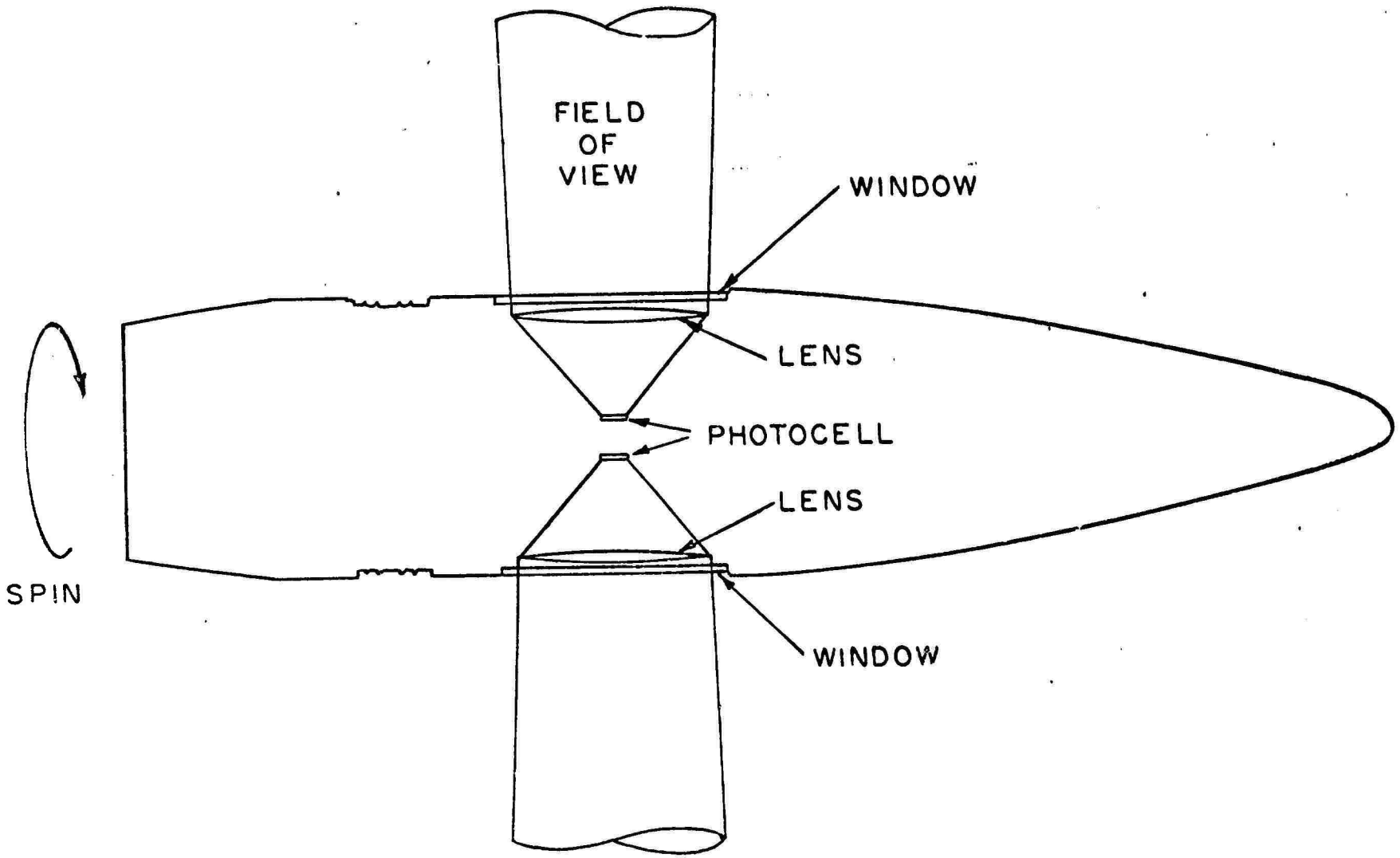

FIGURE 4

SIDE LOOKING CONFIGURATION

launch, to protect the optics while within the artillery tube. Several optical systems would be arranged around the circumference. If the required scan angle were sixty degrees, then six systems would be employed. If a focal length greater than allowed by the shell diameter were required, the optical axes of the six systems could be arranged parallel to the shell axis, and plane mirrors inclined at 45° to the axis would direct the field of view normal to the shell axis.

B. A "forward looking" configuration in which the field of view makes an angle, say 45°, with respect to the axis, see Fig. 5. Here the optical system would be mounted either on the side or nose of the shell. A cap to protect the optics would be discarded after leaving the muzzle. Again, multiple optical systems would be provided. The problem of arranging multiple optical systems around the axis would be more severe than for the side-looking approach.

C. An axial configuration in which the optical axis is aligned with the axis of the shell, see Fig. 6. The optical system would be mounted directly in the nose, with one or more detectors mounted slightly off-axis. This configuration has the advantage of requiring only a single optical system. However, the scan angle must be very limited in order to minimize off-axis distortions including coma. Although a detailed analysis of distortions is beyond the scope of this report, it would appear that the off-axis angle must be no greater than a few degrees. This would severely curtail the utility of the scanner. For this reason, the nose looking configuration is ruled out.

2.2 Discussion

Of the remaining two configurations, the scanning geometry of the side-looking one is the more desirable from the viewpoint of ease of reconstruction of the imagery at the ground station. The field of view of the side-looking configuration can be thought of as a

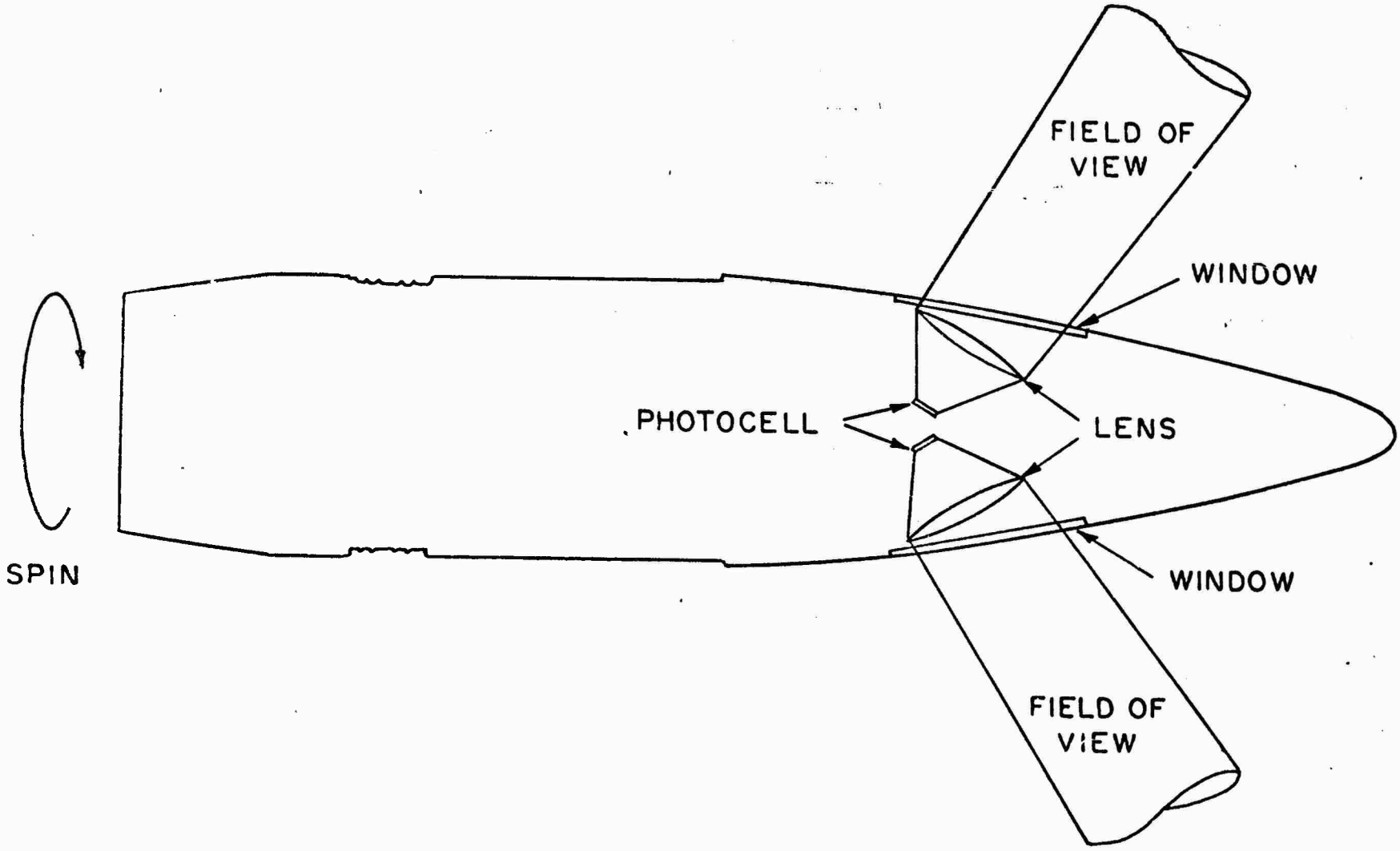

FIGURE 5
FORWARD LOOKING CONFIGURATION

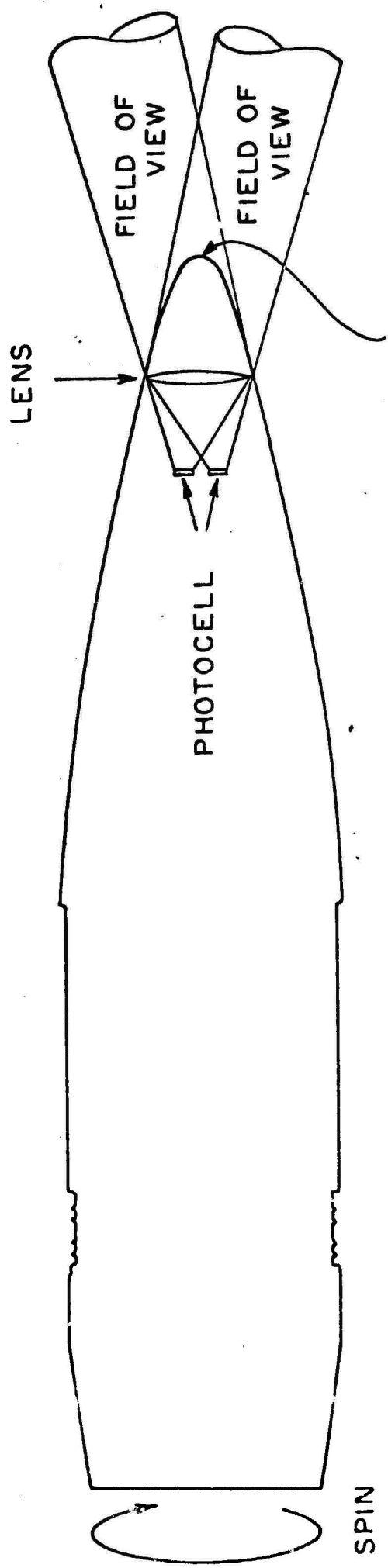

FIGURE 6
AXIAL CONFIGURATION

circular plane concentric with the shell, see Fig. 7. (In reality, the plane is very slightly wedge shaped in cross-section, the wedge angle being the instantaneous angular field of view.) Regardless of the orientation of the shell with respect to the horizontal, the intersection of this plane with the ground plane is a straight line. (It will be seen in Section 3.1.3 that the width of the line varies with distance from the center.)

On the other hand, the field of view of the forward looking one is a cone whose apex is along the centerline of the shell. (Here too, there is a slight wedge-shape.) The intersection of this cone with the ground plane is an ellipse, a straight line, or a parabola. Which of these geometrical figures it is depends upon the instantaneous value of the angle which the shell makes with respect to the horizontal, see Figs. 8 and 9. Because the angle changes continuously during flight, the shapes of these figures change with each scan during flight.

Reconstruction on the ground of the forward looking imagery is difficult. The most direct way would be to employ a reflecting cone whose half angle is the same as the angle which the optical system makes with the shell axis. Radiation from a point light source whose intensity is modulated by the electrical signal telemetered from the shell would be reflected from the cone to fall upon a sheet of photographic film placed horizontally below the cone. The angle which the cone makes with respect to the film plane would be changed with time in a manner coincident with that which the shell in flight makes with respect to the ground plane. In this analogue method of imagery reconstruction, the path of the radiation from the lamp to the film would be similar to the path from the earth plane to the detector. Thus the modulated radiation reflected to the film by the cone would trace out ellipses and parabolas similar to those scanned by the shell on the earth.

3.0 PERFORMANCE CALCULATIONS

Calculations of the system performance can be divided into those relating to geometrical considerations and those relating to photometric considerations. In the analysis which follows, it will be assumed that the side-looking configuration is employed. The previous discussion

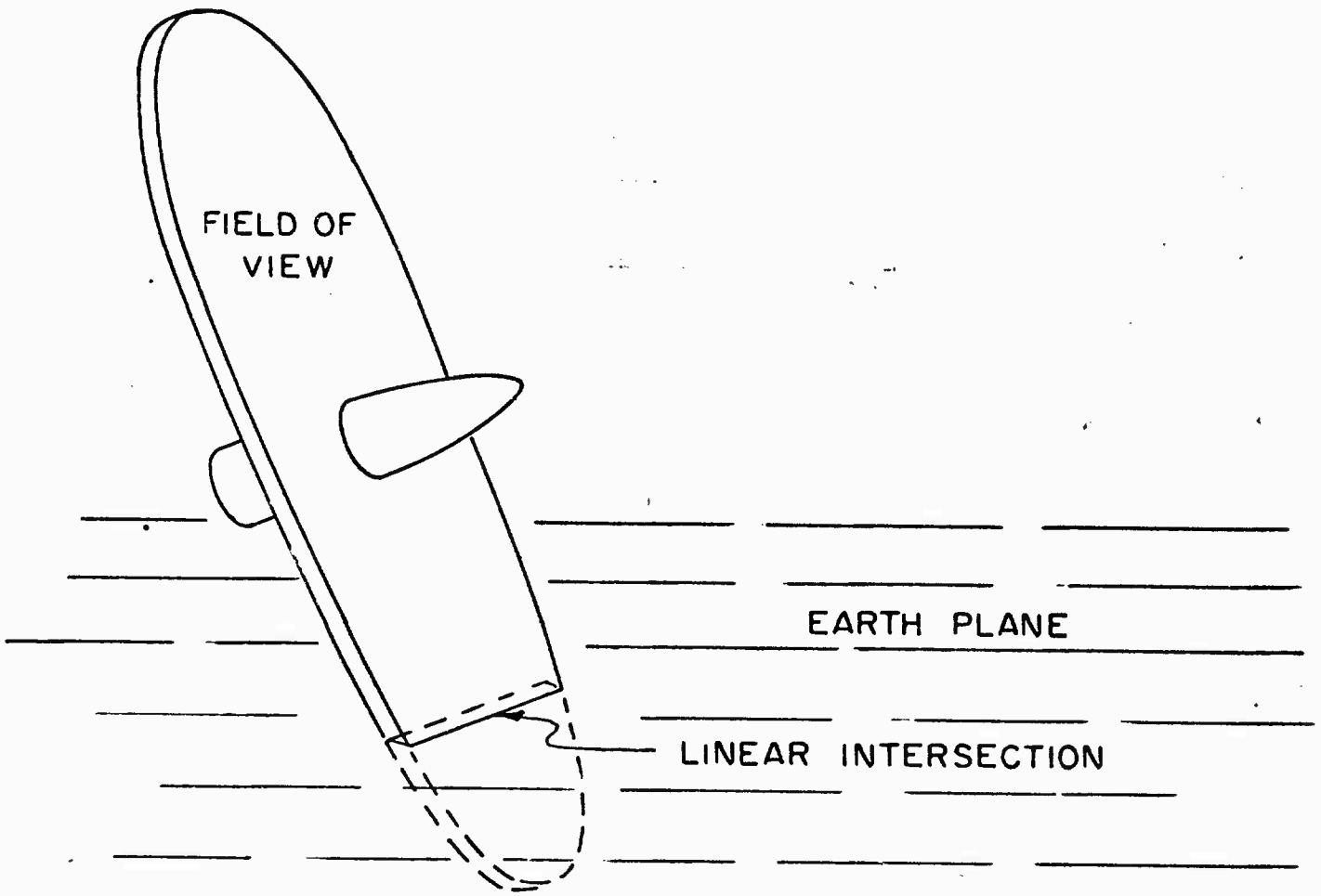

FIGURE 7

INTERSECTION OF FIELD OF VIEW OF SIDE LOOKING CONFIGURATION WITH EARTH PLANE

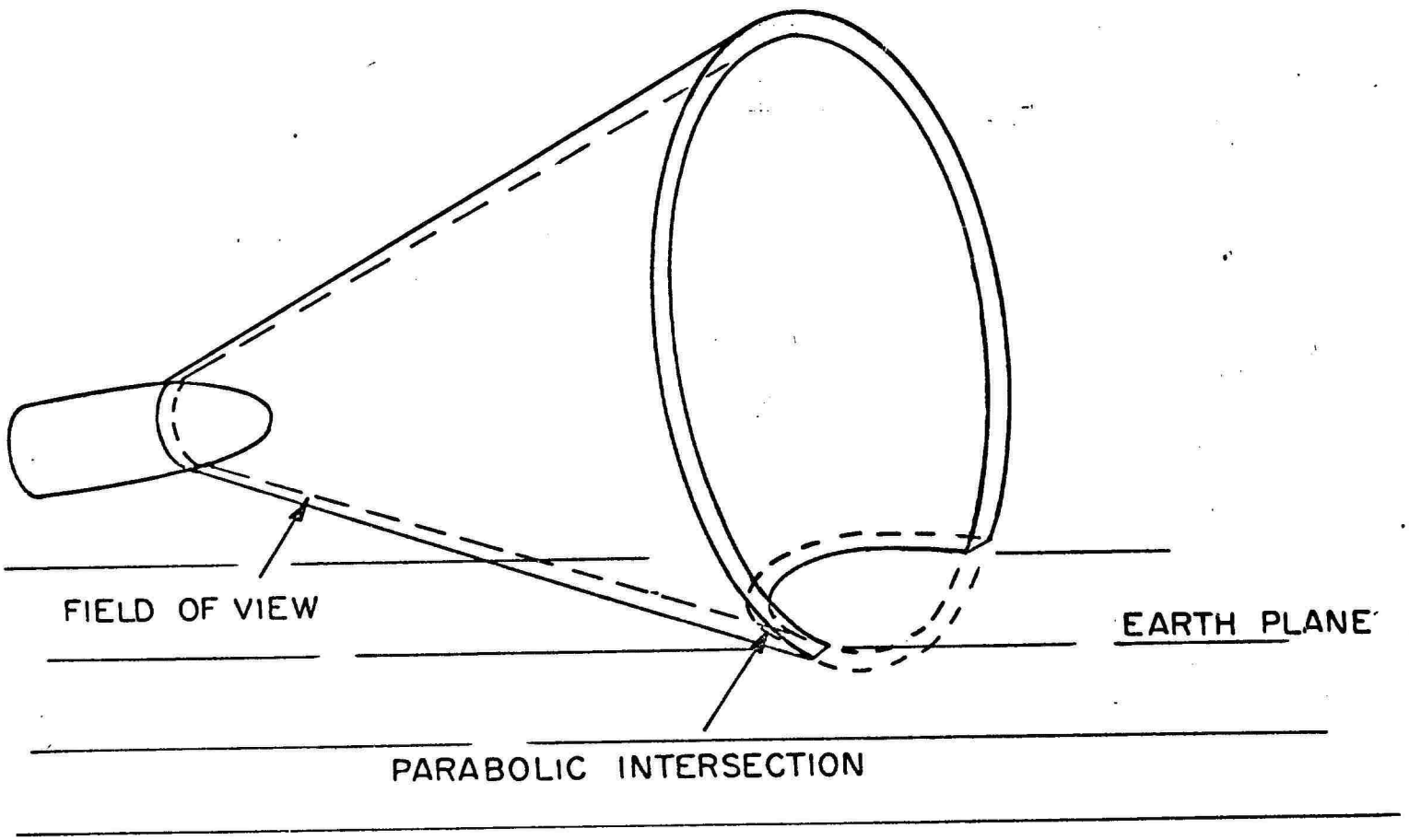

FIGURE 8

INTERSECTION OF FIELD OF VIEW OF FORWARD LOOKING CONFIGURATION WITH EARTH PLANE – PARABOLIC CASE

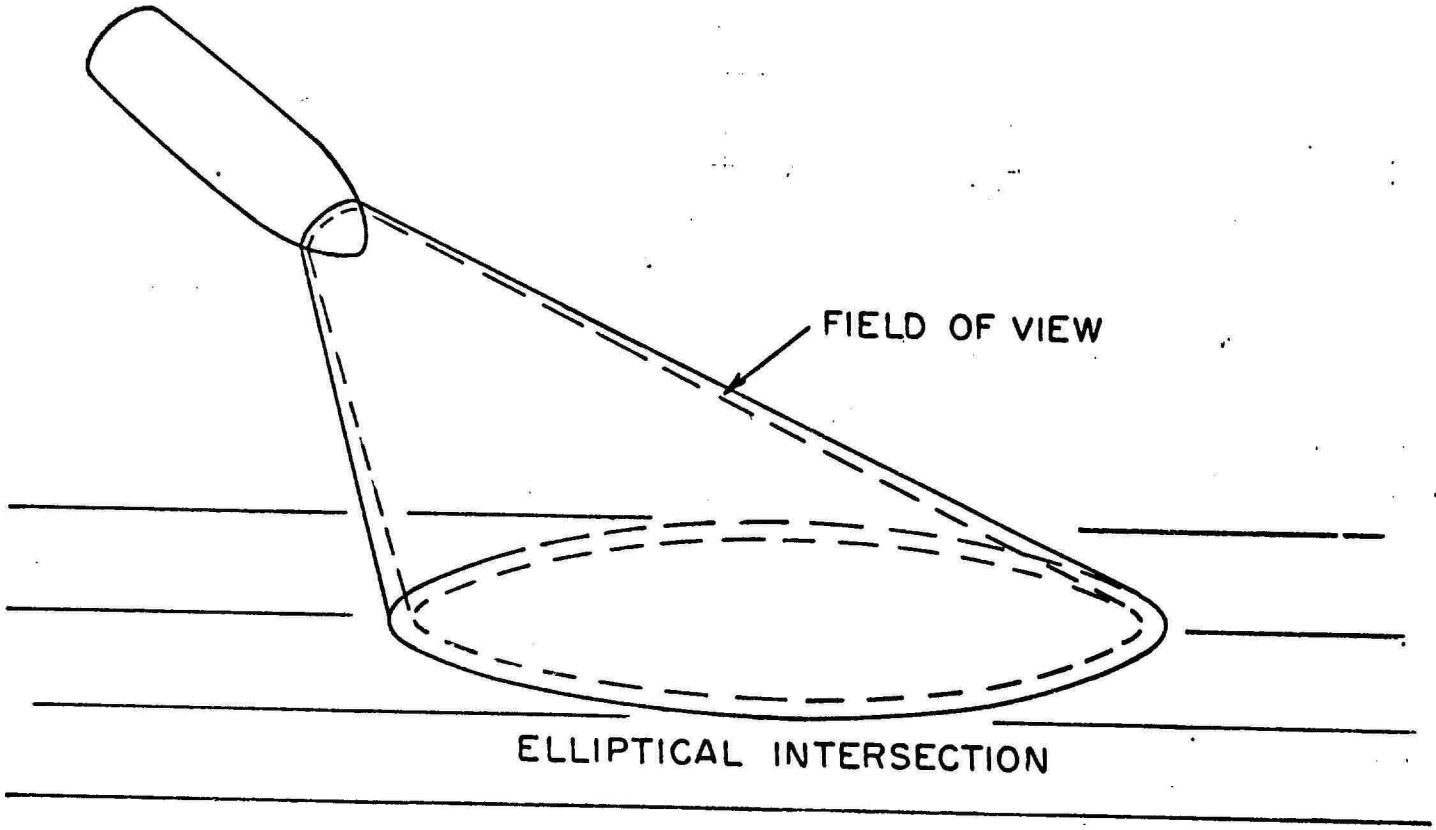

FIGURE 9

INTERSECTION OF FIELD OF VIEW OF FORWARD LOOKING CONFIGURATION WITH EARTH PLANE – ELLIPTICAL CASE

has shown that the geometry of the scan pattern projected upon the ground for the forward looking configuration is an ellipse or parabola whose shape changes continuously with time during flight, whereas that for the side-looking configuration is a straight line, independent of time. Furthermore, the only portion of the trajectory in which it might be desirable to look at a forward angle along the flight path rather than normal to it, would be near impact. Yet it will be seen that mode A operation, in which the time dependences of the parameters entering into the scanning equation tend to compensate, is possible only during the middle portion of the trajectory. Because the forward looking configuration is the more complex, yet has no readily ascertainable advantages, analysis of it will be left to some future date if warranted.

3.1 Geometrical Considerations

3.1.1 Time Independent Contiguous Mapping

Analysis of the scanner geometry is similar to that of an airborne mapper, discussed by Holter and Wolfe.[2] The shell rotates at a rate r revolutions per sec. Let n be the number of optical systems, arranged every 360/n degrees around the axis. At the focal point of each lens let there be a linear array of ℓ detectors, the axis of the array paralleling the shell axis. Let there be ℓ electronic systems operating in parallel. At any instant these electronic systems are individually connected to the detectors in a given array. This array is the one whose optical system is looking downward, rotating through an angle of 360/n about the vertical. The output of each of the ℓ electronic systems is multiplexed to the telemetry transmitter. As the shell rotates, the electronic systems are simultaneously switched from array to array as each array rotates through the identified angle. A timing signal for the switching, provided by a horizon sensor or some other means, is also telemetered to ground.

Assume each detector element is square, having side length p. If the focal length of the lens is f, the instantaneous angular field of view β is given by

$$\beta = \frac{p}{f} . \qquad (1)$$

For the system to produce useful imagery, β should be no greater than 1 milliradian, with 0.1 milliradian preferred.

With each rotation of the shell, ℓ parallel scan lines are swept out on the ground perpendicular to the shell axis. Since the shell axis is tangent to the trajectory, the field of view intercepts the ground at an angle to the normal which equals the angle θ_D of the shell axis with respect to the horizontal. During the initial portion of the trajectory in which the shell is rising toward apogee, the nose up condition causes the optical system to scan the earth plane at a point, termed the track, ahead of the point directly below the shell, i.e., the range. At apogee, when the shell axis is horizontal, the track and range coincide. Beyond apogee, the nose down attitude causes the track to trail the range. The relationship between track and range is given by

$$x = x_o + h \tan\theta_D; \qquad (2)$$

where x is the track and x_o is the range. Values of track as a function of range for the assumed trajectory are listed in Table 2 and plotted in Fig. 10.

Because track and range coincide at launch and also at impact, yet differ in between except at apogee, the track and range velocities must differ. The range velocity is simply the horizontal component of the shell velocity. The track velocity V_T can be computed from the time derivative of the track position. Thus

$$V_T = V_H + V_V \tan\theta_D + h \sec^2\theta_D \frac{d\theta_D}{dt} \; ; \qquad (3)$$

where V_H and V_V are the horizontal and vertical components of the shell velocity.

TABLE 2

VALUES OF PERTINENT
PARAMETERS CALCULATED FROM DATA IN TABLE 1

Time (Seconds)	Horizontal Range (Meters)	Track (Meters)	$\frac{V_T \cos^2 \theta_D}{hr}$	m_o (Meters)	m (Meters)	w_o (Meters)	w (Meters)
0.0	0.0	0	∞	0	0	0	0
2.2	885.8	1701.8	0.003796	0.1187	0.1679	0.1634	0.3269
4.4	1704.4	3137.9	0.001847	0.2159	0.3054	0.2887	0.5775
6.6	2468.7	4347.5	0.001192	0.2947	0.4168	0.3825	0.7651
8.8	3188.1	5353.8	0.0008536	0.3574	0.5054	0.4492	0.8985
11.0	3869.7	6181.4	0.0006451	0.4061	0.5793	0.4940	0.9880
13.2	4519.3	6853.7	0.0005012	0.4430	0.6265	0.5212	1.0425
15.4	5142.8	7384.4	0.0003896	0.4697	0.6643	0.5345	1.0691
17.6	5746.8	7804.7	0.0003117	0.4888	0.6912	0.5389	1.0778
19.8	6337.4	8145.3	0.0002556	0.5021	0.7101	0.5382	1.0764
22.0	6918.3	8402.6	0.0001974	0.5106	0.7221	0.5337	1.0674
24.2	7491.8	8608.5	0.0001618	0.5159	0.7296	0.5285	1.0569
26.4	8058.8	8772.2	0.0001318	0.5189	0.7339	0.5239	1.0478
28.6	8620.0	8901.4	0.0001069	0.5202	0.7358	0.5210	1.0421
30.8	9175.4	9021.0	0.0001021	0.5204	0.7360	0.5206	1.0413
33.0	9725.2	9127.8	0.00009258	0.5197	0.7350	0.5197	1.0394
35.2	10269.5	9236.3	0.00009792	0.5181	0.7327	0.5287	1.0575
37.4	10808.3	9371.8	0.0001230	0.5149	0.7282	0.5362	1.0724
39.6	11341.5	9530.4	0.0001454	0.5100	0.7212	0.5456	1.0911
41.8	11868.9	9740.2	0.0001916	0.5018	0.7097	0.5542	1.1083
44.0	12390.5	9999.8	0.0002377	0.4900	0.6930	0.5614	1.1228
46.2	12905.6	10319.6	0.0002940	0.4735	0.6697	0.5653	1.1306
48.4	13413.4	10729.5	0.0003823	0.4501	0.6366	0.5607	1.1214
50.6	13912.8	11211.3	0.0004643	0.4203	0.5944	0.5487	1.0974
52.8	14401.9	11794.2	0.0005945	0.3816	0.5397	0.5226	1.0453
55.0	14879.0	12479.2	0.0007677	0.3336	0.4718	0.4802	0.9604
57.2	15340.4	13283.4	0.0010515	0.2745	0.3882	0.4151	0.8302
59.4	15790.5	14195.0	0.0025048	0.1646	0.2328	0.2112	0.4225
61.6	16222.0	15243.7	0.0053811	0.09005	0.1273	0.1120	0.2240
63.8	16635.8	16428.8	0.03205	0.01709	0.02417	0.02069	0.04138
64.3	16729.6	16729.6	∞	0	0	0	0

FIGURE 10

INTERSECTION OF FIELD OF VIEW WITH EARTH PLANE (TRACK) AS A FUNCTION OF HORIZONTAL DISTANCE OF SHELL FROM LAUNCH POINT (RANGE)

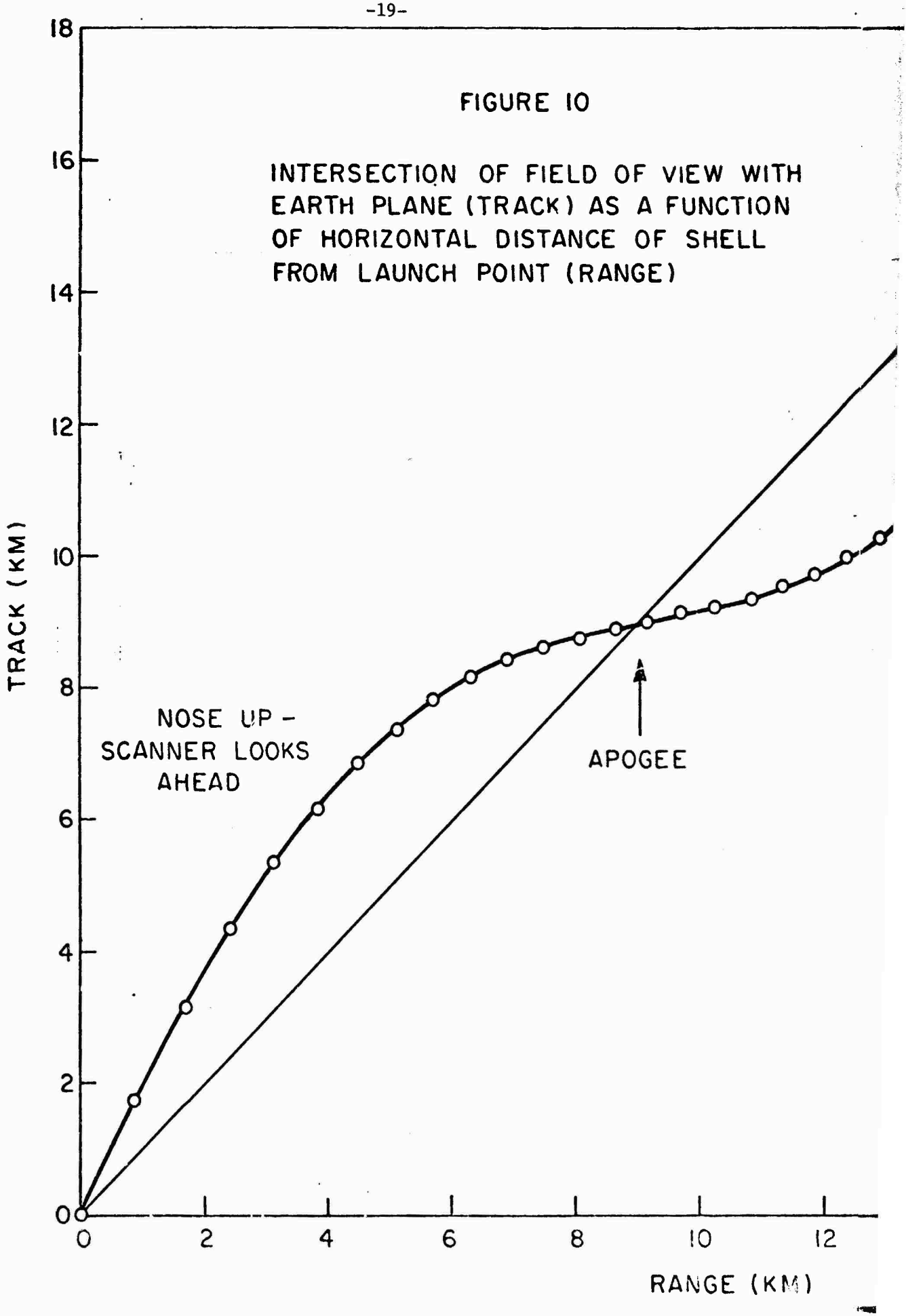

FIGURE 10

ECTION OF FIELD OF VIEW WITH
PLANE (TRACK) AS A FUNCTION
IZONTAL DISTANCE OF SHELL
AUNCH POINT (RANGE)

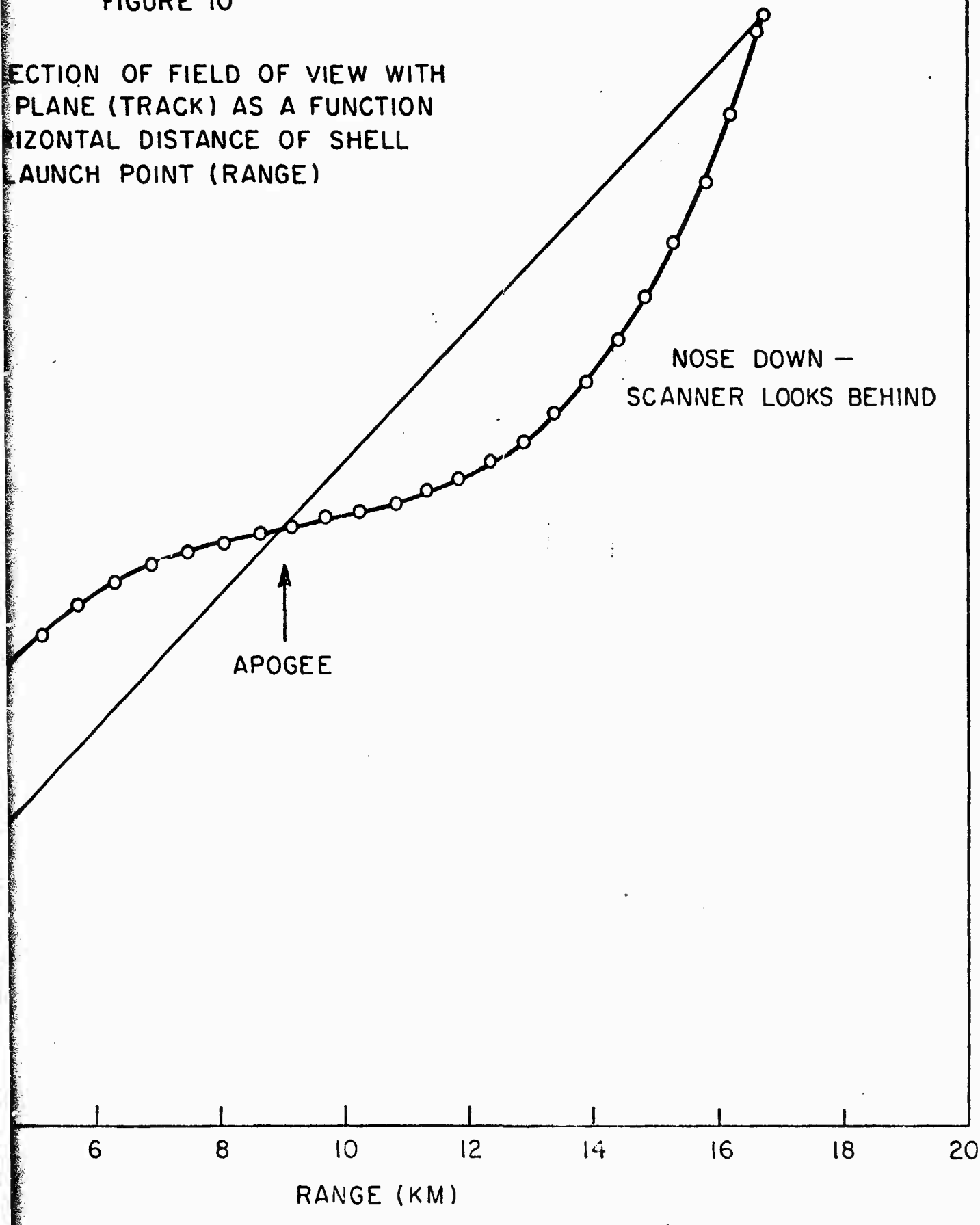

2

The number of lines scanned per revolution is given by $n\ell$, and the number of lines scanned per second is given by $n\ell r$. Assume that the scanning action must be contiguous, so that the lines are neither underlapped nor overlapped. Then the horizontal distance traveled by the field of view per second must equal the total width of the lines on the ground per second. The width w_o of each line upon the ground is given by

$$w_o = \beta h \sec^2\theta_D. \tag{4}$$

Thus

$$V_T = \beta h n \ell r \sec^2\theta_D; \tag{5}$$

Rearranging gives

$$\beta n \ell = \frac{V_T \cos^2\theta_D}{hr}. \tag{6}$$

The left side of Eq. (6) contains parameters whose values cannot be changed during flight. The instantaneous field of view β, determined by the size of the detector and the focal length of the lens, the number of optical systems, and the number of elements in the array are all predetermined. The right hand side contains ballistic parameters whose values are constantly changing during flight. The right hand side can only equal the left hand side at more than one instant of time if the time dependences of V_T, h, r, and θ_D compensate each other in the ratio.

The ratio contained in the right hand side of Eq. (6), calculated from the ballistic data of Table 1, is listed in Table 2 and plotted as a function of range in Fig. 11.

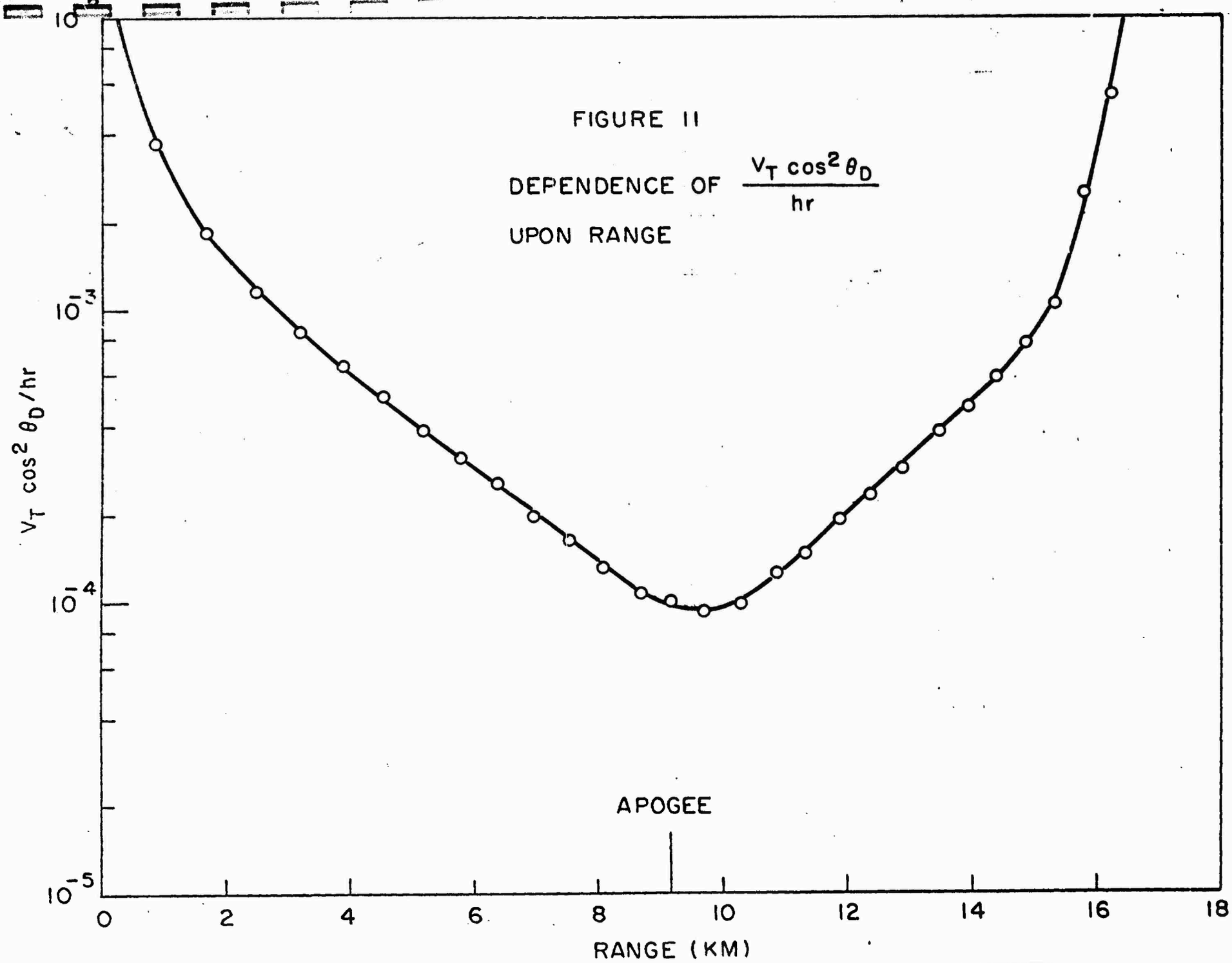

FIGURE 11

DEPENDENCE OF $\frac{V_T \cos^2 \theta_D}{hr}$

UPON RANGE

The ratio changes continuously during flight, first decreasing, then increasing past apogee. Only near apogee is it relatively independent of range. The same conclusion is reached if the forward looking configuration rather than the side looking one is employed, since the only change is to increase the aspect angle θ_D by a fixed amount.

It is thus clear that for the assumed trajectory the requirement for time independent contiguous mapping cannot be met over an appreciable portion of the trajectory. There is, however, a portion near apogee of approximately 1 kilometer length in which the requirement is essentially met, i.e., in which the function plotted in Fig. 11 is nearly constant with range and track. Thus the spinning round scanner can be employed over the assumed trajectory by firing it such that the target of interest is below it at apogee. With flatter trajectories it would seem that the useable portion of the trajectory near apogee would be greater than 1 kilometer.

Consider now the magnitude of the system parameters. Figure 11 shows that in the useable range near apogee the ratio on the right hand side of Eq. (6) is approximately 1×10^{-4}. Experience dictates that a desirable value of β is of the order of 0.1 milliradian. Thus the $n\ell$ product should be unity, which can only be achieved through having $n = 1$ and $\ell = 1$. In other words, contiguous mapping can be achieved by having one detector and one optical system. In practice, however, four optical systems, each with one detector, would be a better choice, each responsible for a 90° sector. Although this would lead to fourfold overlap in the imagery, this should not be a serious problem. Indeed overlap can sometimes be employed to increase the signal-to-noise ratio.

It is necessary to verify that the diffraction limit is not exceeded. This is given by

$$\beta_D = 1.22\lambda/D; \tag{7}$$

where λ is the wavelength of the radiation and D is the diameter of the optics. Since the system is designed to operate in the visible portion of the spectrum, λ is approximately 5×10^{-4}cm. D must be much less than the diameter of the 203mm round, so assume D to be 8cm. Then

$$\beta_D \simeq 8 \times 10^{-6} \text{ radians.}$$

Thus the system envisioned is more than an order of magnitude away from the diffraction limit, which is certainly sufficient.

The detector side length is given by Eq. (1). Assuming an f/2 optical system, then f ≃ 16cm and $p \simeq 1.6 \times 10^{-3}$cm. Although preparing a detector element whose side length is 16μm is difficult, it is within the state of the art wher photolithographic methods are employed.

3.1.2 Dwell Time

Contiguous mapping is not the only constraint upon the system parameters. It is also necessary that the scanner dwell on each resolution element a time of at least $k\tau$, where k is a small number, say two, and τ is the detector time constant. The dwell time is given by the reciprocal of the number of elements scanned per second, i.e., by $(2\pi r/\beta)^{-1}$. Thus

$$\frac{\beta}{2\pi r} > k\tau; \tag{8}$$

or

$$r < \frac{\beta}{2\pi k\tau}. \tag{9}$$

The ratio on the right of Eq. (9) involves the time independent system parameters β and τ, whereas r on the left changes with time during flight. Since r decreases monotonically with time, the inequality is preserved throughout the flight if it is obeyed at launch.

Because the detector time constant has not yet been determined, the inequality can be employed to set an upper limit to it. The value of β has

been determined to be 1×10^{-4} radians. Assume k = 2. Table 1 shows that r at launch is 117 rev/sec (735 rad/sec). Then the inequality shows that

$$\tau < 6.7 \times 10^{-8} \text{sec.}$$

The maximum allowable value of τ is therefore 67 nsec.

3.1.3 Ground Resolution

A parameter of obvious interest is the ground resolution. At a given altitude and aspect angle, the intersection of the instantaneous field of view with the ground plane determines the ground resolution. As developed in Eq. (4), the width w_o of each line in the direction of the flight path and along the flight path depends upon $\sec^2\theta_D$. The length m_o of each resolution element in the direction perpendicular to the flight path along the path is given by

$$m_o = \beta h \sec\theta_D. \tag{10}$$

To either side of the flight path, both w and m increase. From Fig. 12 it can be seen that

$$w = w_o \sec^2\phi = \beta h \sec^2\theta_D \sec^2\phi; \tag{11}$$

and

$$m = m_o \sec\phi = \beta h \sec\theta_D \sec\phi; \tag{12}$$

where ϕ is the scan angle to either side of the normal. Assuming the value of n = 4 then $\phi = 45°$.

Figure 13 illustrates the ground resolution as a function of range for the assumed trajectory. The values of w_o and m_o have been computed from Eqs. (4) and (10) using the data from Table 1, and the value of $\beta = 1 \times 10^{-4}$ previously determined. The values of w and m were determined from Eqs. (11) and (12), using also the data of Table 1 and assuming $\beta = 1 \times 10^{-4}$. Furthermore, the value of $\phi = 45°$ has been assumed, so that the w and m values represent the resolution at the extreme end of each scanning line for a scanner having four optical systems, i.e., for n = 4.

FIGURE 12

SCANNING GEOMETRY
PERPENDICULAR TO FLIGHT PATH

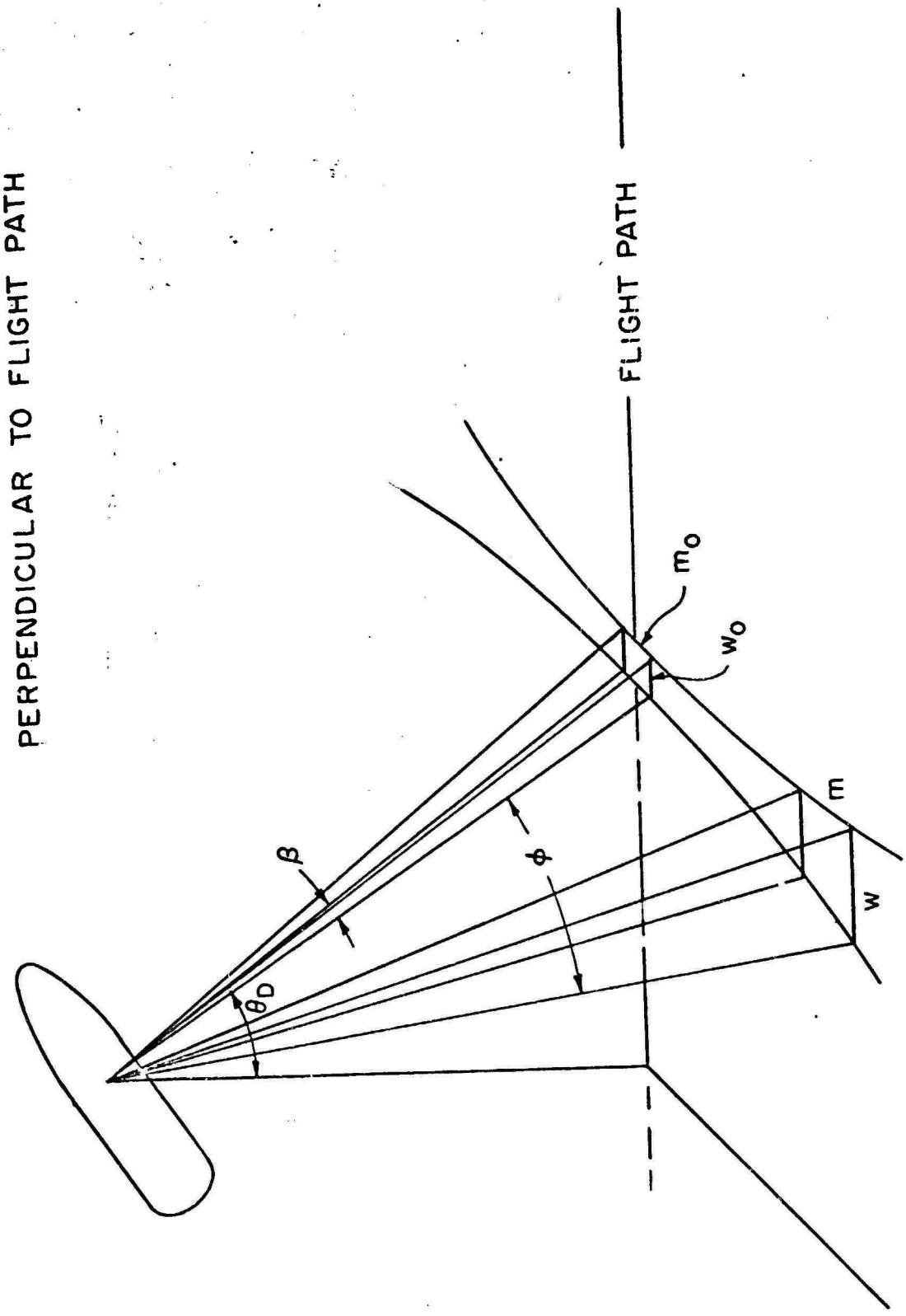

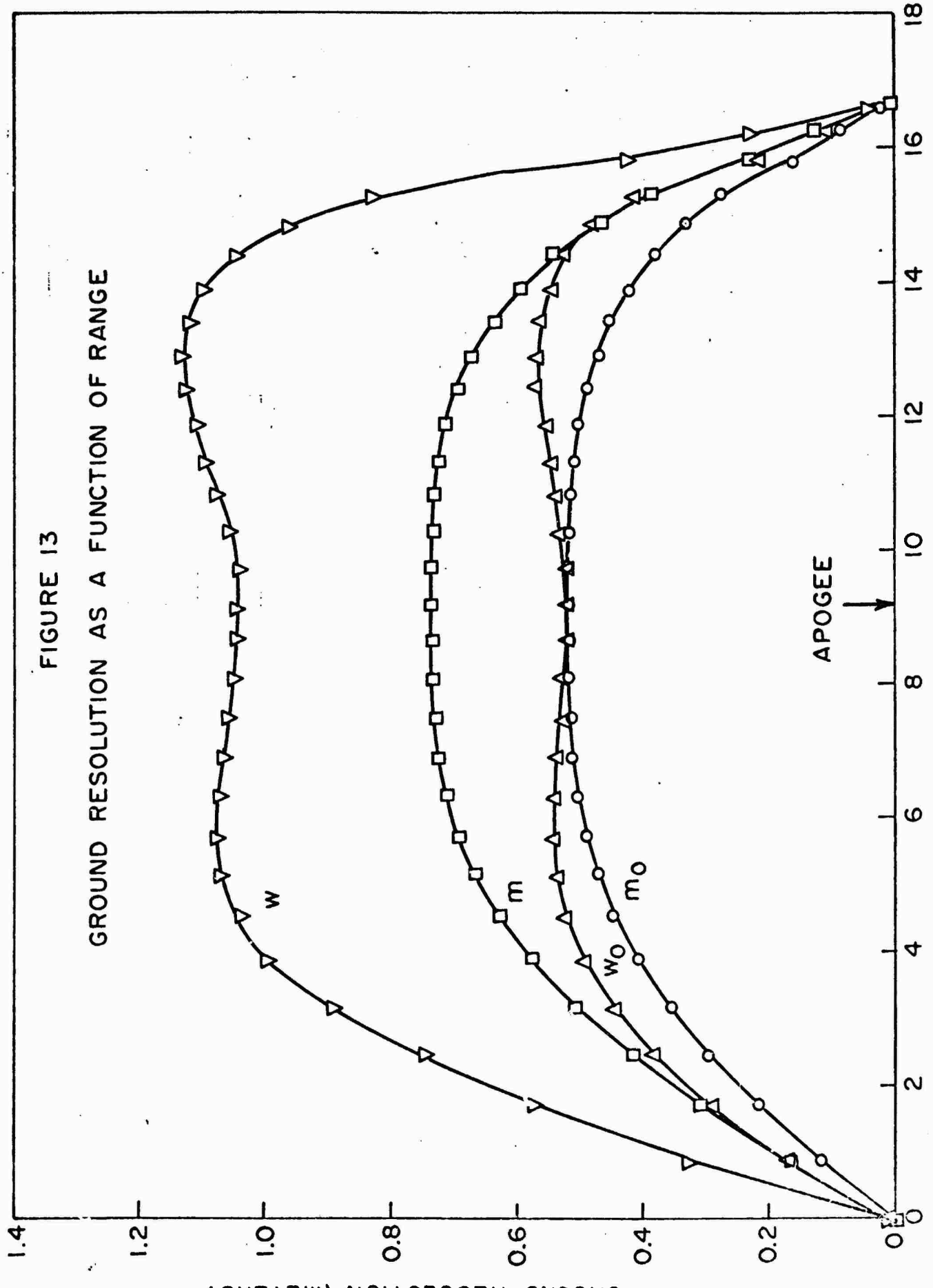

FIGURE 13

GROUND RESOLUTION AS A FUNCTION OF RANGE

This is also consistent with the previous conclusions. Values of w_o, w, m_o, and m can be found in Table 2.

Figure 13 shows that the ground resolution below the shell along the flight path is no poorer than about 0.54 meters in the direction of flight (w_o) and about 0.52 meters perpendicular to the direction of flight (m_o). These maximum values of resolution are attained near apogee and decrease slowly on either side of apogee. Furthermore, the maximum (poorest) resolution at the extreme edges of the scan, i.e., for $\phi = 45°$, is approximately 1.08 meters in the direction of flight and 0.74 meters perpendicular to the flight path.

Since the time independent contiguous mapping requirement is only achieved near apogee, the appropriate ground resolution values are those near apogee, which is the poorest case. Neverthelsss, the values quoted above compare favorably with those obtainable from airborne reconnaissance imagery. They are certainly adequate for targets such as vehicles, roads, buildings,and groups of individuals.

3.2 Photometric Considerations

The previous section addressed the geometrical requirements relating to contiguous mapping. The signal-to-noise voltage ratio and minimum detectable contrast are the subjects of the present section. It is assumed that the spin stabilized round is fired during a clear sunny day. The terrain is assumed to be a flat Lambertian (perfectly diffuse) reflector characterized by an average reflectivity ρ which is wavelength independent over the spectral interval to which the photocell responds. Point-to-point variations in the reflectance which characterize the imagery are given by $\Delta\rho$. The signal-to-noise voltage ratio for a given average reflectivity will be determined in terms of the solar irradiance, photocell properties, and optical system. The minimum detectable contrast, i.e., the normalized minimum detectable change in reflectivity, will be determined. Measured properties of silicon photocells will be introduced into the performance equations to determine numerical values of the signal-to-noise voltage ratio and threshold contrast.

3.2.1 Properties of Silicon Photocells

The spinning round scanner requires a low cost photocell. The dwell time analysis indicated a very fast response was needed. The obvious choice is a silicon (Si) photodiode. The properties of Si photodiodes are reviewed below. These data have been compiled from that supplied by various manufacturers[3] plus measurements reported by Naval Weapons Center, Corona.[4]

The photocell is characterized[5] by its spectral detectivity, D^*_λ, its solar detectivity, $D^*(T_S)$, and its response time, τ. The spectral detectivity is the output signal-to-noise voltage ratio measured in a 1 Hz bandwidth at a given center frequency in response to 1 watt of monochromatic radiant power of a given wavelength. The solar detectivity is the output signal-to-noise voltage ratio measured in a 1 Hz bandwidth at a given center frequency in response to 1 watt of solar radiation. The response time is defined in several ways; one is that point on the modulation frequency response characteristic at which the signal voltage has fallen to 0.71 of its value in the low frequency plateau.

A typical spectral response is illustrated in Fig. 14. The value of D^*_λ at the spectral peak at 0.9μm is 2×10^{12} cm $Hz^{1/2}$/watt. Also illustrated is the spectral distribution of sunlight. From these two curves, the conversion factor[6] from $D^*_\lambda(0.9\mu m)$ to $D^*(T_S)$ is found to be 3.3. Thus the value of $D^*(T_S)$ is 6×10^{11} cm $Hz^{1/2}$/watt.

The response time of a Si photodiode can be limited by either the time for photoexcited hole-electron pairs to transit the depletion region of the junction or by the $R_L C$ product, where R_L is the load resistance and C is the junction plus package capacitance. With the very small junction areas required for the intended application, the junction and package capacitance would be sufficiently small so that for reasonable makes of R_L the frequency response would be limited by the electron-hole transit time. In general, this would be of the order of 10 nsec, certainly meeting the 67 nsec requirement determined earlier.

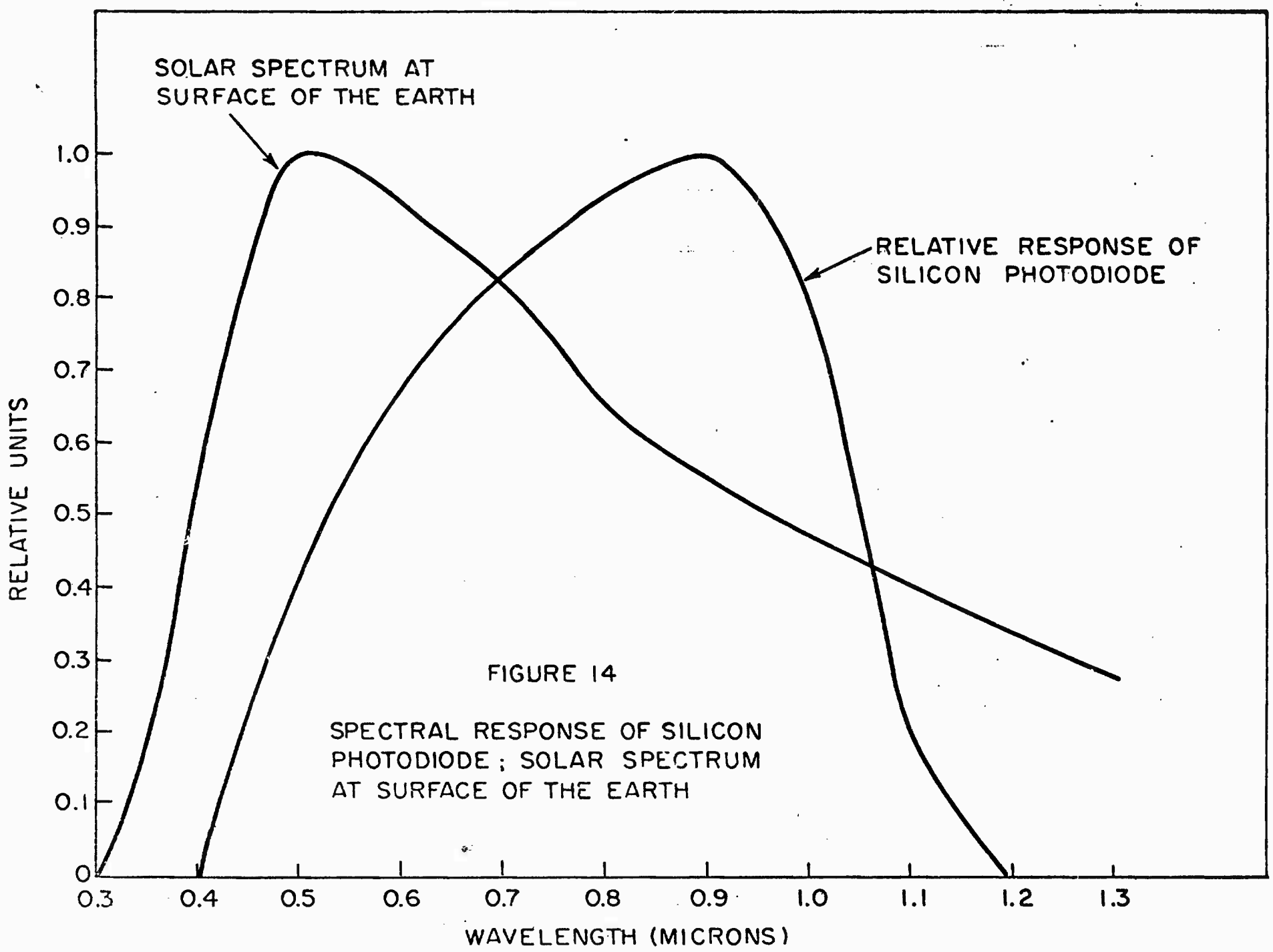

FIGURE 14

SPECTRAL RESPONSE OF SILICON PHOTODIODE ; SOLAR SPECTRUM AT SURFACE OF THE EARTH

3.2.2 Signal-to-Noise Ratio and Minimum Detectable Contrast

Consider the geometry illustrated in Fig. 15. Sunlight falling upon the terrain with an irradiance (radiant power per unit area) of H is reflected by the surface in a Lambertian manner, described by a cosine distribution about the normal. The photocell at the focal point of the optical system within the spinning round views the terrain through a solid angle β^2 at an angle of incidence θ_D along the path of length R. Assume that at a given instant the area A_S on the terrain intercepted by the solid angle β^2 is on the flight path, rather than to one side of it. Then

$$A_S = \frac{(\beta R)^2}{\cos\theta_D} . \tag{13}$$

The radiant intensity J, i.e., the radiant power per unit solid angle centered about the angle θ_D, is given by

$$J = \frac{\rho H A_S \cos\theta_D}{\pi} \tag{14}$$

where the factor π rather than 2π in the denominator arises from the Lambertian reflecting nature of the terrain. The radiant power P intercepted by the lens having diameter D is then given by

$$P = \frac{J\pi D^2 T}{4R^2} ; \tag{15}$$

where T is the transmission of the atmosphere over the path length R averaged over the spectral interval of interest.

Combining Eqs. (13) - (15) results in

$$P = \frac{\rho H \beta^2 D^2 T}{4} . \tag{16}$$

Thus the radiant power falling on the photocell is proportional to the terrain irradiance and reflectance, the solid angle β^2 through which the photocell views the terrain, the area of the lens, and the atmospheric transmittance. It is independent of the aspect angle θ_D; the cosine distribution of the Lambertian reflector just cancels the cosine dependence of the reflecting surface area upon θ_D.

FIGURE 15

GEOMETRY FOR PHOTOMETRIC ANALYSIS

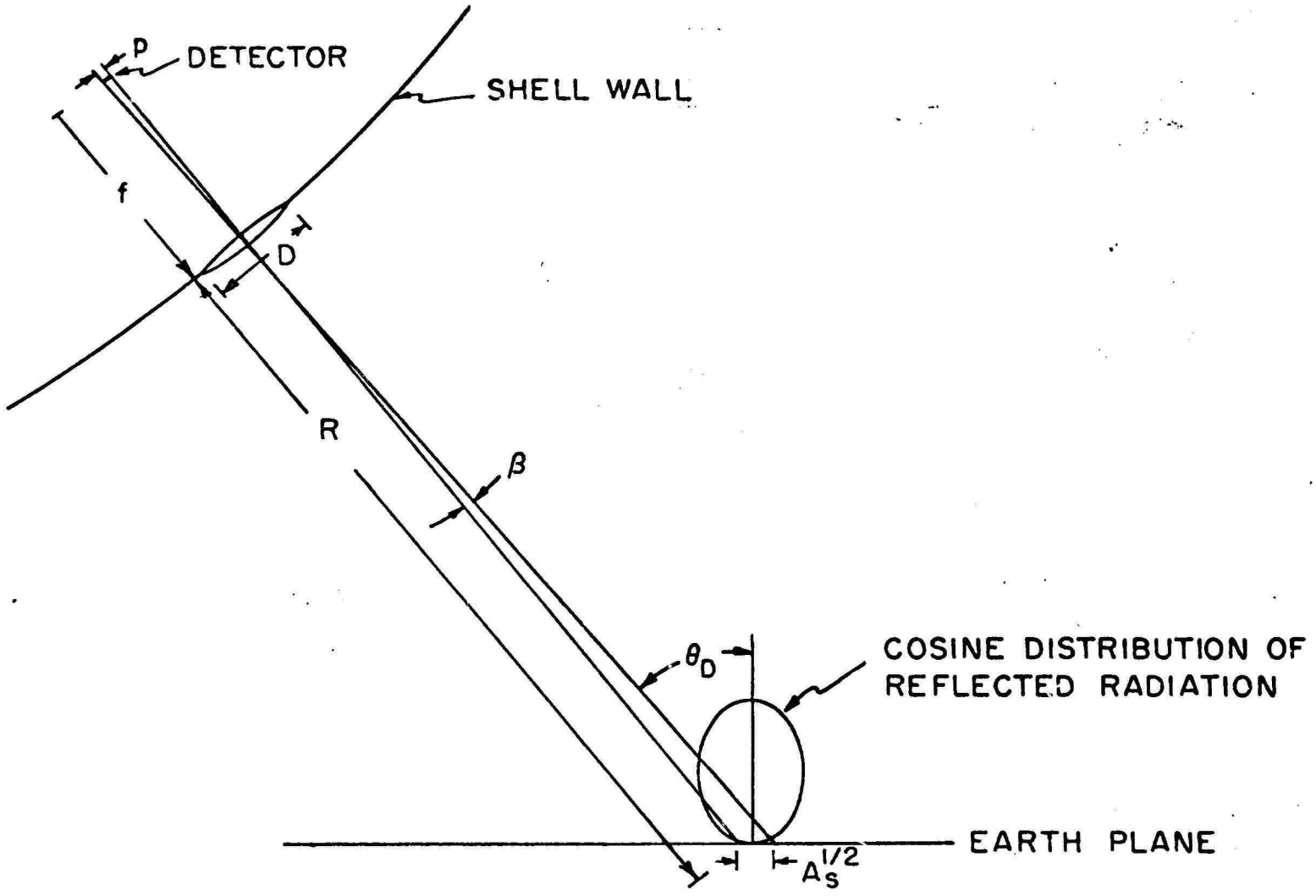

An alternative expression for P is obtained by introducing F, the f/number of the lens,

$$F = \frac{f}{D} . \tag{17}$$

Combining this with the expression for β, Eq. (1), allows Eq. (16) to be rewritten as

$$P = \frac{\rho H p^2 T}{4F^2} \tag{18}$$

where p^2 is the area of the detecting element of the photocell.

The signal-to-noise voltage ratio in the output from the photocell is given by

$$\left(\frac{v_S}{v_N}\right) = \frac{PD^*(T_S)}{pB^{1/2}} ; \tag{19}$$

where B is the bandwidth in which the signal-to-noise is measured. (The noise voltage is proportional to the square root of the bandwidth). The bandwidth is determined at its upper limit by the dwell time τ. Its lower limit will be of the order of 100 Hz, to minimize the contribution from 1/f power law noise. Thus, for all intents and purposes,

$$B = \frac{1}{2\pi\tau} ; \tag{20}$$

For τ= 67 nanoseconds, B = 2.38MHz. Combining Eqs. (16),(19), and (20) results in

$$\left(\frac{v_S}{v_N}\right) = \frac{\rho H \beta^2 D^2 T D^*(T_S)}{4pB^{1/2}} . \tag{21}$$

Equation (21) describes the signal-to-noise voltage ratio in the photocell output in response to sunlight reflected from terrain having an average reflectivity ρ. This expression does not provide for contrast in the scene. In reality, the imagery is reconstructed from small variations Δp in the reflectance. Without these, the scene would be uniformly bright, devoid of detail.

Thus, a figure of merit of particular interest is the minimum detectable contrast, C_{min}, defined as that minimum contrast in the scene which gives rise to a signal just equal to the noise within the bandwidth B. Since contrast is defined as

$$C = \frac{\Delta\rho}{\rho} ; \tag{22}$$

C_{min} is determined by solving Eq. (23) for that value of $\Delta\rho$ required to give rise to a signal-to-noise voltage ratio of unity, then dividing by the average reflectivity ρ. Thus

$$C_{min} = \frac{4pB^{1/2}}{\rho H\beta^2 D^2 TD^*(T_S)} \tag{23}$$

which is just the reciprocal of the signal-to-noise voltage ratio.

Note the Eqs. (21) and (23) do not contain explicitely any trajectory parameters. The signal-to-noise voltage ratio and the minimum detectable contrast are independent of range , altitude, and aspect angle, except insofar as the atmospheric transmittance T depends slowly upon range. It can be seen that the path length R and angle θ_D both cancel in the expression for the radiant power P falling on the photocell, Eq. (16).

The theoretical values of the signal-to-noise voltage ratio and minimum detectable contrast can now be determined. The irradiance of sunlight outside the atmosphere (solar constant) is 0.14 watts/cm^2. Because of atmospheric absorption over the wavelength interval of interest, the irradiance H at the surface of the earth on a cloudless day will be approximately 0.09 watts/cm^2. The reflectance ρ of terrain varies widely over the earth, but a representative value in the spectral interval of interest is 0.1. A representative value for the lens diameter D is 8 cm. It has already been shown that a reasonable choice for β is 1.0×10^{-4} radians, and that $p = 1.6 \times 10^{-3}$cm. The transmission of the atmosphere is assumed to vary only slowly with path length. Over the spectral interval and path lengths of interest its value is estimated at 0.8. The value of solar detectivity $D^*(T_S)$ is 6×10^{11}cm $Hz^{1/2}$/watt. The value of the bandwidth B is assumed to be 2.38 MHz.

Inserting these values into Eq. (21), the signal-to-noise voltage ratio is found to be

$$\frac{v_S}{v_N} = 280.$$

Similarly, the minimum detectable contrast is

$$C_{min} = 0.00357.$$

Thus, with values of the parameters consistent with the problem, the predicted signal-to-noise voltage ratio is 280, and the minimum detectable contrast is 0.36%. In other words, a reflectivity change of 0.36% of the average reflectivity of 10%, or an absolute reflectivity change of 0.036%, is detectable.

The values of signal-to-noise voltage ratio and minimum detectable contrast permit high quality imagery under clear sky daylight operational conditions. Operation under cloudy conditions, in which the irradiance is reduced by one order of magnitude, is even possible, since the signal-to-noise voltage ratio and minimum detectable contrast depend linearly upon the irradiance. That is to say, under an overcast sky, the signal-to-noise voltage ratio would be 28, and the minimum detectable contrast would be 0.0357. Of course, the cloud layer must not be between the scanner and the earth, so the cloud ceiling must be higher than the apogee, since time independent contiguous mapping is possible only near apogee for the trajectory under consideration.

4.0 DISCUSSION AND SUMMARY

This report constitutes an initial examination of the concept of employing an expendable spin stabilized artillery round containing a simple optical system and telemetry equipment to obtain reconnaissance imagery. The analysis considers the geometric and photometric requirements, including time independent contiguous mapping, signal to noise ratio, and minimum detectable contrast. Equations are derived having general applicability. In order to obtain numerical values of the appropriate system performance parameters, data for a 203mm round fired due north from the equator at a 45° elevation with a zone seven charge have been employed. There is nothing unique about this trajectory; it was simply one provided to illustrate the calculations. Indeed, it appears that a lower elevation with a flatter trajectory would have been a better choice.

Three configurations for the scanner were initially considered, an axial one, a forward looking one, and a side looking one. The axial one was ruled out because of its limited field of view. The forward looking one was not considered in detail because it introduces excess complexity. That is to say, the intersection of the field of view with the earth plane is a series of parabolas and ellipses whose parameters change continuously during flight.

The side looking configuration has been examined in detail. The requirement for time independent contiguous mapping, summarized by Eq.(6), is applicable to all trajectories. Introducing the assumed trajectory data, Table 1, it is found that the contiguous mapping requirement is satisfied during an interval of about 1 kilometer near apogee. Actually, the requirement is not really satisfied, since the scanning lines will overlap. However, the ground based imagery reconstruction system can accommodate the excess information provided by overlap, whereas it cannot of course supply the missing information had underlap been the problem.

The ground resolution has been examined both along the track and perpendicular to it. Equations (4), (10), (11), and (12) expressing it are generally applicable to all trajectories. By introducing the assumed trajectory data, the resolution at apogee was found to be

roughly 0.5 meters square along the track, increasing to about 0.7 x 1.1 meters at the maximum distance perpendicular to the crack (45° off-axis). These values should certainly be adequate for imagery of vehicles, road, buildings, and groups of personnel. It may be possible to exploit the overlap to obtain imagery of even higher resolution.

The analysis also showed that the optical system could be very simple, four lenses arranged at 90° intervals about the shell circumference, each with a single silicon photocell at the focal point.

The photometric requirements have been examined in detail. Equations (21) and (23), generally applicable, describe the signal-to-noise voltage ratio and the minimum detectable optical contrast. The trajectory does not enter explicitely into the photometric considerations since the path length and aspect angle both cancel in the expression for the optical power reaching the photocell.

By inserting values of solar irradiance appropriate to a clear day, the signal-to-noise voltage ratio and minimum detectable contrast have been numerically evaluated. These values assure excellent performance under sunlit conditions. It appears that even with an overcast sky, the performance would be very good. Of course, the optical system cannot "see"through" clouds; the round would have to be fired below the cloud layer.

In summary, then, it appears from this initial examination that the spinning round concept is feasible, or at least it has not been shown to be not feasible. The photometric requirements can be met during daylight operation, even beneath clouds. The time independent contiguous mapping requirement for the assumed trajectory can be met over a distance of about one kilometer near apogee. Presumably the requirement can be met over an even greater distance for a flatter trajectory. In operation, the shell would be fired such that the targets of interest lay below the shell at apogee. The ground resolution so obtained would certainly be adequate for many targets of interest.

5.0 RECOMMENDATIONS

Because this initial study has shown the concept to be a promising one, further studies are warranted. Among these are the following:

Other Trajectories

Examine other trajectories to see whether the contiguous mapping requirement can be met over a distance greater than 1 kilometer. Rather than employing numerical data in the form given in Table 1, combine the trajectory equations with the contiguous mapping and ground resolution equations, then solve directly to obtain plots similar to Figs. 11 and 13.

Synch Signal

A synch signal is required to trigger each scan line in the ground based receiver. Some device such as an on-board horizon scanner is needed. Determine the synch signal requirements and examine possible techniques for meeting them.

Telemetry System

The telemetry system has been ignored. Explore the initial configuration of the on-board transmitter and ground based receiver.

Imagery Reconstruction Equipment

Explore the requirements and configuration of the ground based equipment employed for imagery reconstruction.

Shock & Vibration

From sources of information such as Project HARP examine whether the electronic and optical systems can withstand the firing shock.

Lab Experiments

Simulate the scanner by breadboarding the optical system, mounting

it on a turntable to provide the scanning action, providing a controlled optical input representing sunlit terrain, and examining the electrical output from the photocell.

Initial On-Board System Layout

Consider how to configure the optical and electrical equipment for various rounds such as the 155mm, 175mm, and 203mm ones.

System Cost

Obtain a rough cost estimate of the expendable round and the ground based equipment.

Applications

Determine the military use of the system, given its performance and limitations, for the 155mm, 175mm, and 203mm rounds.

Alternative Approach

Examine the feasibility of the mode B approach wherein the time dependent parameters including altitude, aspect angle, velocity, and spin rate are continuously monitored and their values telemetered to the ground based receiver to be used in the imagery reconstruction equipment. Determine whether the additional complexity and cost is a valid tradeoff for being able to obtain useful imagery over the entire trajectory.

it on a turntable to provide the scanning action, providing a controlled optical input representing sunlit terrain, and examining the electrical output from the photocell.

Initial On-Board System Layout

Consider how to configure the optical and electrical equipment for various rounds such as the 155mm, 175mm, and 203mm ones.

System Cost

Obtain a rough cost estimate of the expendable round and the ground based equipment.

Applications

Determine the military use of the system, given its performance and limitations, for the 155mm, 175mm, and 203mm rounds.

Alternative Approach

Examine the feasibility of the mode B approach wherein the time dependent parameters including altitude, aspect angle, velocity, and spin rate are continuously monitored and their values telemetered to the ground based receiver to be used in the imagery reconstruction equipment. Determine whether the additional complexity and cost is a valid tradeoff for being able to obtain useful imagery over the entire trajectory.